

# Journal of Mechanics of Materials and Structures

BOUNDARY INTEGRAL EQUATION FOR  
NOTCH PROBLEMS IN AN ELASTIC HALF-PLANE  
BASED ON GREEN'S FUNCTION METHOD

Y. Z. Chen

Volume 7, No. 10

December 2012



## BOUNDARY INTEGRAL EQUATION FOR NOTCH PROBLEMS IN AN ELASTIC HALF-PLANE BASED ON GREEN'S FUNCTION METHOD

Y. Z. CHEN

This paper studies a boundary integral equation (BIE) for notch problems in an elastic half-plane based on Green's function method. The boundary along the half-plane is traction-free. A fundamental solution is suggested, which is composed of a principal part and a complementary part. The process for evaluating the complementary part from the principal part is similar to the Green's function method for Laplace's equation. After using the Somigliana identity or Betti's reciprocal theorem between the field of the fundamental solution and the physical field, the displacements at the domain point are obtained. Letting the domain point approach the boundary point and using the generalized Sokhotski–Plemelj formula, a BIE of the notch problem for a traction-free half-plane boundary is obtained. The accuracy of the suggested technique is examined. Computed results for elliptic notches and a square notch with rounded corner are presented in the paper.

### 1. Introduction

It is well known that except for in some simple cases the solution for elastic problems cannot be obtained in a closed form. Therefore, researchers research the numerical solutions of elastic problems. In fact, some boundary integral equations (BIEs) in plane elasticity were suggested in [Muskhelishvili 1953]. However, even though some integral equations could then be formulated, it was difficult to solve them using simpler computation instruments, such as by hand. The situation changed significantly after the computer became available. Researchers developed two important computation techniques in elasticity: the finite element method and the boundary integral equation method.

Boundary integral equations (BIEs) in elasticity were proposed by several pioneer researchers [Rizzo 1967; Cruse 1969; Jaswon and Symm 1977]. The history of the development of BIEs was summarized recently in [Cheng and Cheng 2005]. In the direct formulation of BIEs, the dual formulations are significant. In the first version of the BIE, the boundary displacements are related to the boundary displacement and traction through some integral operators. In the second version of the BIE, the boundary tractions are related to the boundary displacement and traction through some integral operators. Generally, the singularity of the kernels of the second version is higher by one order than its counterpart in the first version [Brebbia et al. 1984; Hong and Chen 1988].

The use of complex integral equations has some proven advantages for solving two-dimensional potential and elastic problems [Hromadka and Lai 1987; Linkov and Mogilevskaya 1994; Mogilevskaya and Linkov 1998; Linkov 2002; Chen and Chen 2004]. Recently, a formulation of indirect BIEs in plane elasticity using single or double layer potentials and complex variables was suggested [Chen et al. 2010].

*Keywords:* elasticity, elastic half-plane, notch problem, fundamental solution, Green's function method, complex variable BIE.

Continuous and discontinuous properties of the displacements and tractions of a moving point across the boundary play an important role in the formulation of BIEs. These properties can be investigated exactly through the use of complex variables.

The stress concentration problem around a notch is an important topic in the strength of materials. Many problems in this field were solved in [Savin 1961]. However, the scale of study and accuracy of computation in early year (1951) was not expected, simply because no modern computer was available at that time. A special boundary element formulation for multiple circular hole problems in an infinite plate was suggested in [Chen 1985]. The multiple circular hole problem for an elastic half-plane and the periodic group circular hole problems were solved by using the series expansion variational method [Chen 1994; Chen and Lin 2007].

An analytical solution has been given for the class of problems of an elastic half plane with a circular cavity loaded on the cavity boundary. For the case of a uniform radial stress at the cavity boundary the solution can be given in a closed form [Verruijt 1998]. A complex boundary integral equation method has been presented for the problem of an infinite isotropic elastic plane containing multiple circular holes. The suggested method was reduced to solve a hypersingular integral equation [Wang et al. 2003]. It is seen from the derivation that the method is effective for solving the problem of multiple circular holes. Similarly, a semianalytical method was presented for solving the problem of an isotropic elastic half-plane containing multiple circular holes of arbitrary sizes [Dejoie et al. 2006]. A boundary element formulation for cracked anisotropic elastic half-planes was proposed. In the formulation, the complex potentials were composed of two parts, a principal part and a complementary part [Chen and Cheung 1990; Pan et al. 1997].

This paper studies a boundary integral equation for notch problems in an elastic half-plane based on Green's function method. The boundary along the half-plane is traction-free. The first step in the derivation is to formulate a fundamental solution. In the usual BIE, the fundamental solution corresponds to a particular solution for concentrated forces applied at a point. Thus, this solution does not satisfy the traction-free condition along the boundary of the half-plane.

In the present study, the pair of complex potentials for concentrated forces in the usual formulation is called the principal part, and is denoted by  $\phi_p(z)$  and  $\psi_p(z)$ . The complex potentials for the traction-free half-plane boundary can be investigated in the form of  $\phi(z) = \phi_p(z) + \phi_c(z)$  and  $\psi(z) = \psi_p(z) + \psi_c(z)$ . The purpose of introducing the part composed of  $\phi_c(z)$  and  $\psi_c(z)$  is to eliminate the tractions along the half-plane boundary caused by  $\phi_p(z)$  and  $\psi_p(z)$ . The pair of complex potentials  $\phi_c(z)$  and  $\psi_c(z)$  is called the complimentary part in the whole complex potentials. The pair  $\phi_c(z)$  and  $\psi_c(z)$  can be derived from the pair  $\phi_p(z)$  and  $\psi_p(z)$  in an exact way, which is similar to the Green's function method in the solution of Laplace's equation. After using the Somigliana identity or Betti's reciprocal theorem between the field of the fundamental solution and the physical field, the displacements at the domain point are obtained. Letting the domain point approach the boundary point and using the generalized Sokhotski–Plemelj formula, a BIE for notch problems for a traction-free half-plane boundary is obtained. Since the fundamental solution satisfies the traction-free condition along the boundary of the half-plane in advance, there is no need to set the equation for points along the half-plane boundary. The formulation is a general one, without regard to the configuration of the notch. A discretization procedure is suggested, and the accuracy of the suggested method is examined. Computed results for elliptic notches and a square notch with rounded corners are presented in the paper.

**2. Formulation of BIE for notch problems in an elastic half-plane based on Green’s function method**

**Background on the complex variable method of plane elasticity.** The complex variable function method plays an important role in plane elasticity. The fundamentals of this method are introduced here. In the method, the stresses  $(\sigma_x, \sigma_y, \sigma_{xy})$ , the resultant forces  $(X, Y)$  and the displacements  $(u, v)$  are expressed in terms of complex potentials  $\phi(z)$  and  $\psi(z)$  such that [Muskhelishvili 1953]

$$\sigma_x + \sigma_y = 4 \operatorname{Re} \phi'(z), \quad \sigma_y - \sigma_x + 2i\sigma_{xy} = 2[\bar{z}\phi''(z) + \psi'(z)], \tag{1}$$

$$f = -Y + iX = \phi(z) + z\overline{\phi'(z)} + \overline{\psi(z)}, \tag{2}$$

$$2G(u + iv) = \kappa\phi(z) - z\overline{\phi'(z)} - \overline{\psi(z)}, \tag{3}$$

where a bar over a function denotes the conjugated value for the function,  $G$  is the shear modulus of elasticity,  $\kappa = (3 - \nu)/(1 + \nu)$  in the plane stress problem,  $\kappa = 3 - 4\nu$  in the plane strain problem, and  $\nu$  is the Poisson’s ratio. Sometimes, the displacements  $u$  and  $v$  are denoted by  $u_1$  and  $u_2$ , the stresses  $\sigma_x$ ,  $\sigma_y$ , and  $\sigma_{xy}$  by  $\sigma_1$ ,  $\sigma_2$ , and  $\sigma_{12}$ , and the coordinates  $x$  and  $y$  by  $x_1$  and  $x_2$ . For the sake of the following derivations, an equation for finding a particular derivative is introduced as follows [Muskhelishvili 1953; Savruk 1981; Chen et al. 2003]:

$$\frac{d}{dz}\{f(z)\overline{g(z)}\} = f'(z)\overline{g(z)} + \frac{d\bar{z}}{dz}(f(z)\overline{g'(z)}). \tag{4}$$

In (4),  $f(z)$  and  $g(z)$  denote some analytic functions. The derivative in (4) is called the derivative in a specified direction (DISD).

Except for the physical quantities mentioned above, from (2) and (3) two DISDs are introduced as follows [Savruk 1981; Chen et al. 2003]:

$$J_1(z) = \frac{d}{dz}\{-Y + iX\} = \phi'(z) + \overline{\phi'(z)} + \frac{d\bar{z}}{dz}(z\overline{\phi''(z)} + \overline{\psi'(z)}) = \sigma_N + i\sigma_{NT}, \tag{5}$$

$$J_2(z) = 2G\frac{d}{dz}\{u + iv\} = \kappa\phi'(z) - \overline{\phi'(z)} - \frac{d\bar{z}}{dz}(z\overline{\phi''(z)} + \overline{\psi'(z)}) = (\kappa + 1)\phi'(z) - J_1. \tag{6}$$

It is easy to verify that  $\sigma_N$  and  $\sigma_{NT}$  in  $J_1 = \sigma_N + i\sigma_{NT}$  denote the normal and shear tractions along the segment from  $z$  to  $z + dz$ . Secondly, the  $J_1$  and  $J_2$  values depend not only on the position of a point  $z$ , but also on the direction of the segment  $d\bar{z}/dz$ .

The physical meaning of  $J_1(z) = d/dz\{-Y + iX\} = \sigma_N + i\sigma_{NT}$  and  $J_2(z) = 2Gd/dz\{u + iv\}$  is introduced in Figure 1. Since  $-Y + iX$  (see (2)) represents the resultant force function defined along the interval from  $z$  to  $z + dz$  (Figure 1), we can prove

$$J_1(z) = \frac{d}{dz}\{-Y + iX\} = \lim_{dz \rightarrow 0} \frac{\{-Y + iX\}|_{\text{at } z+dz} - \{-Y + iX\}|_{\text{at } z}}{dz} = \sigma_N + i\sigma_{NT}. \tag{7}$$

Thus, the  $J_1(z)$  value represents the traction  $\sigma_N + i\sigma_{NT}$  applied along the interval from  $z$  to  $z + dz$  (Figure 1).

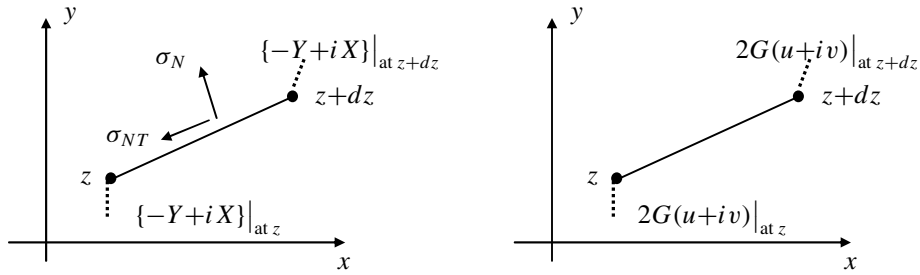


**Figure 1.** Left: physical meaning of the component  $J_1(z)$ . Right: physical meaning of the component  $J_2(z)$ .

Similarly, since  $2G(u + iv)$  represents the displacement function defined along the interval from  $z$  to  $z + dz$ , we can define

$$J_2(z) = 2G \frac{d}{dz} \{u + iv\} = 2G \lim_{dz \rightarrow 0} \frac{(u + iv)|_{at\ z+dz} - \{u + iv\}|_{at\ z}}{dz}. \tag{8}$$

Thus, the  $J_2(z)$  value represents the deformation state along the interval from  $z$  to  $z + dz$  (Figure 1). In fact, from the value of  $J_2(z)$ , we can get the elongation and the rotation of the interval from  $z$  to  $z + dz$ .

We can find a particular usage of (5) for work done by two stress fields. Suppose there are two stress fields, which are denoted by the subscripts  $\alpha$  and  $\beta$ . Thus, we can formulate the following equality:

$$(u - iv)^{(\alpha)} (-i J_1^{(\beta)}(z)) dz = (u - iv)^{(\alpha)} d(X + iY)^{(\beta)} \tag{9}$$

and

$$\text{Re}\{-i(u - iv)^{(\alpha)} J_1^{(\beta)}(z) dz\} = u^{(\alpha)} dX^{(\beta)} + v^{(\alpha)} dY^{(\beta)}. \tag{10}$$

Equation (10) represents the work done along the interval from  $z$  to  $z + dz$  for displacement for the  $\alpha$  field to the traction for the  $\beta$  field. Equation (10) is particularly important in the case of using Betti's reciprocal theorem between two stress fields.

**Formulation of BIE for notch problems in an elastic half-plane.** The formulation of a fundamental solution plays an important role in the formulation of BIE for notch problems in an elastic half-plane. The fundamental solution satisfies the following conditions (see Figure 2, top left):

- (1) There is a singular point  $z = \tau$  in the upper half-plane with a concentrated force  $(P_x, P_y)$ .
- (2) The solution satisfies the traction-free condition along the boundary of the half-plane.

The original problem depicted in Figure 2, top left, can be considered as a superposition of the two stress fields defined by the diagrams in the right column of Figure 2. Therefore, it is natural to find the complex potentials for the fundamental solution in the form

$$\phi(z) = \phi_p(z) + \phi_c(z), \quad \psi(z) = \psi_p(z) + \psi_c(z). \tag{11}$$

In (11), the pair  $\phi_p(z)$  and  $\psi_p(z)$  is called the principal part of the whole complex potentials, which is related to the fundamental field caused by concentrated force at the point  $z = \tau$  of the upper half-plane

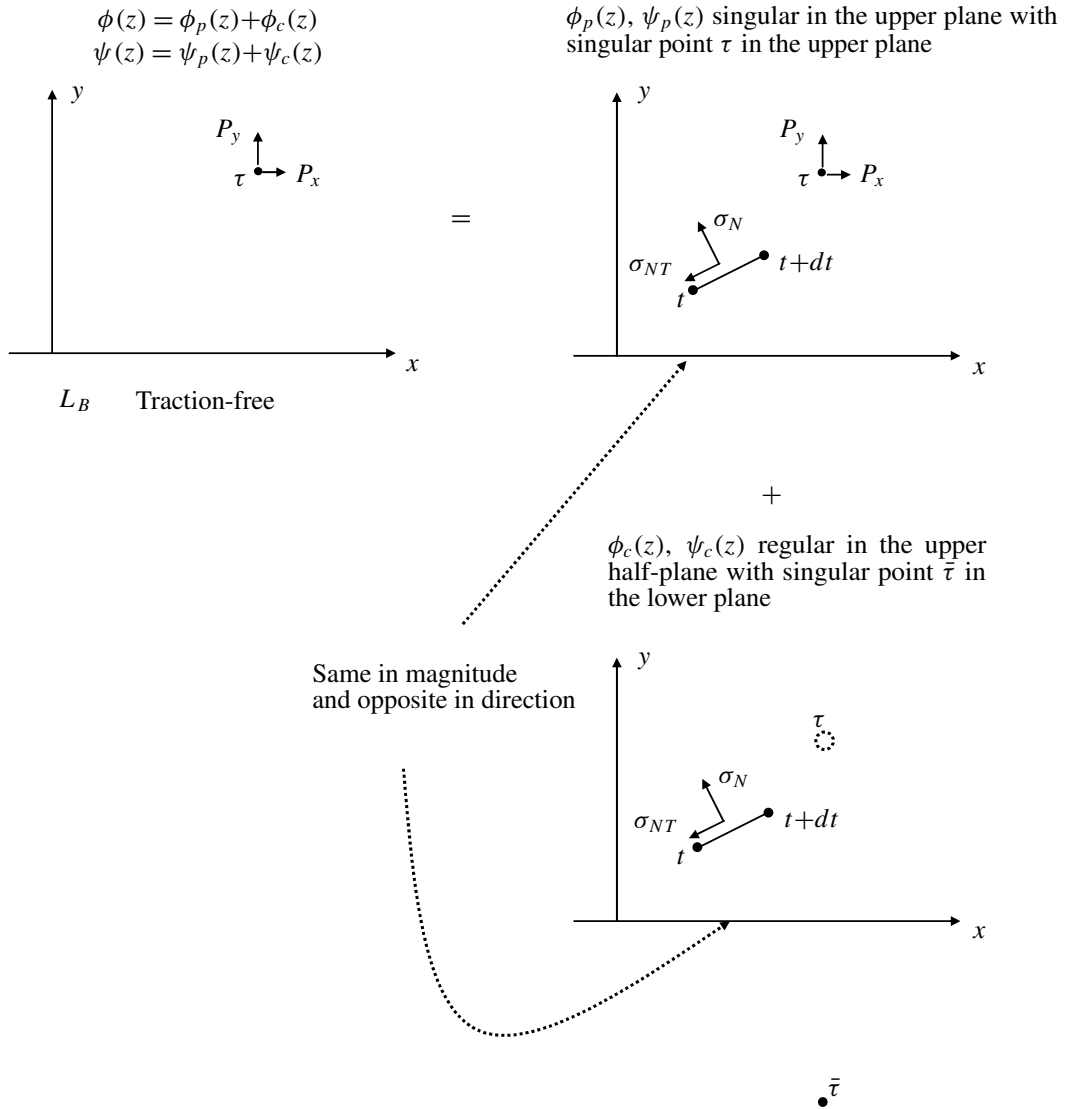


**Figure 2.** Construction of the fundamental solution.

(Figure 2, top right). The relevant complex potentials are as follows [Muskhelishvili 1953; Savruk 1981; Chen et al. 2003]:

$$\phi_p(z) = F \ln(z - \tau), \quad \phi'_p(z) = \frac{F}{z - \tau}, \quad \phi''_p(z) = -\frac{F}{(z - \tau)^2}, \tag{12}$$

$$\psi_p(z) = -\kappa \bar{F} \ln(z - \tau) - \frac{F \bar{\tau}}{z - \tau}, \quad \psi'_p(z) = -\frac{\kappa \bar{F}}{z - \tau} + \frac{F \bar{\tau}}{(z - \tau)^2}, \tag{13}$$

where

$$F = -\frac{P_x + iP_y}{2\pi(\kappa + 1)}. \tag{14}$$

In (14),  $P_x + iP_y$  is the concentrated force applied at the point  $z = \tau$  in Figure 2, top right.

The complex potentials shown by (12) and (13) are defined in the full infinite plane. From (5), (12), and (13) we can evaluate the relevant boundary traction at the point  $t$  with the increase  $dt$  as follows:

$$(\sigma_N + i\sigma_{NT})_{*p} = \frac{F}{t-\tau} + \frac{\bar{F}}{\bar{t}-\bar{\tau}} + \frac{d\bar{t}}{dt} \left( -\frac{\kappa F}{\bar{t}-\bar{\tau}} - \frac{\bar{F}(t-\tau)}{(\bar{t}-\bar{\tau})^2} \right). \quad (15)$$

Similarly, from (3), (12), and (13), we can evaluate the relevant displacement at point  $t$  as follows:

$$2G(u - iv)_{*p} = 2\kappa \bar{F} \ln|t - \tau| - F \frac{\bar{t} - \bar{\tau}}{t - \tau}. \quad (16)$$

In (15) and (16), the subscript  $*p$  denotes that the arguments are derived from the principal part of the complex potentials. It is emphasized here that the pair  $\phi_p(z)$  and  $\psi_p(z)$  does not satisfy the traction-free condition along the boundary of the half-plane  $L_b$  (Figure 2).

In (11), the pair  $\phi_c(z)$  and  $\psi_c(z)$  is called the complementary part, or the regular part, of the whole complex potentials (Figure 2, bottom). The role of the pair  $\phi_c(z)$  and  $\psi_c(z)$  is to eliminate the boundary traction along the boundary of the half-plane caused by the pair  $\phi_p(z)$  and  $\psi_p(z)$  (Figure 2, right column).

Since  $z$  has a real value along the boundary of the half-plane, we have

$$z = \bar{z} \quad (\text{for } z \in L_B). \quad (17)$$

In (17),  $L_B$  denotes the boundary of the half-plane (Figure 2).

It is seen that the traction-free condition along the boundary of the half-plane (or  $\sigma_N + i\sigma_{NT} = 0$ ) along  $z \in L_B$  is equivalent to the vanishing resultant force function along the same boundary (Figure 2). By using (2) and (17), this condition can be expressed as

$$\overline{\phi(z)} + z\phi'(z) + \psi(z) = 0 \quad (\text{for } z \in L_B), \quad (18)$$

or, in an alternative form,

$$\overline{\phi_p(z)} + \overline{\phi_c(z)} + z\phi'_p(z) + \psi_p(z) + z\phi'_c(z) + \psi_c(z) = 0 \quad (\text{for } z \in L_B). \quad (19)$$

Similarly to the image method in electrostatics, substituting (12) and (13) into (19) yields

$$\begin{aligned} \phi_c(z) &= \kappa F \ln(z - \bar{\tau}) + \frac{\bar{F}(\tau - \bar{\tau})}{z - \bar{\tau}}, & \phi'_c(z) &= \frac{\kappa F}{z - \bar{\tau}} - \frac{\bar{F}(\tau - \bar{\tau})}{(z - \bar{\tau})^2}, \\ \phi''_c(z) &= -\frac{\kappa F}{(z - \bar{\tau})^2} + \frac{2\bar{F}(\tau - \bar{\tau})}{(z - \bar{\tau})^3}, \end{aligned} \quad (20)$$

and

$$\begin{aligned} \psi_c(z) &= -\bar{F} \ln(z - \bar{\tau}) - \frac{\kappa F \bar{\tau}}{z - \bar{\tau}} + \frac{\bar{F}(\tau - \bar{\tau})}{z - \bar{\tau}} + \frac{\bar{F}(\tau - \bar{\tau})\bar{\tau}}{(z - \bar{\tau})^2}, \\ \psi'_c(z) &= -\frac{\bar{F}}{z - \bar{\tau}} + \frac{\kappa F \bar{\tau}}{(z - \bar{\tau})^2} - \frac{\bar{F}(\tau - \bar{\tau})}{(z - \bar{\tau})^2} - \frac{2\bar{F}(\tau - \bar{\tau})\bar{\tau}}{(z - \bar{\tau})^3}. \end{aligned} \quad (21)$$

The relevant derivation for obtaining the pair  $\phi_c(z)$  and  $\psi_c(z)$  from the pair  $\phi_p(z)$  and  $\psi_p(z)$  can be found in [Savruk 1981; Chen and Cheung 1990; Chen et al. 2003; 2009]. The complex potentials  $\phi_c(z)$

and  $\psi_c(z)$  have a singular point  $z = \bar{\tau}$  at the lower half-plane, or they represent a regular function in the upper half-plane (Figure 2, bottom right).

From (5), (20), and (21), we can evaluate the relevant traction at the point  $t$  with increasing  $dt$  ( $dt$  a complex value) as follows (Figure 2):

$$(\sigma_N + i\sigma_{NT})_{*c} = \bar{F}c_1(t, \tau) + Fc_2(t, \tau), \tag{22}$$

where

$$\begin{aligned} c_1(t, \tau) &= -\frac{\tau - \bar{\tau}}{(t - \bar{\tau})^2} + \frac{\kappa}{\bar{t} - \tau} - \frac{d\bar{t}}{dt} \frac{\kappa(t - \tau)}{(\bar{t} - \tau)^2}, \\ c_2(t, \tau) &= \frac{\kappa}{t - \bar{\tau}} + \frac{\tau - \bar{\tau}}{(\bar{t} - \tau)^2} + \frac{d\bar{t}}{dt} \left( -\frac{1}{\bar{t} - \tau} + \frac{\tau - \bar{\tau}}{(\bar{t} - \tau)^2} - \frac{2(t - \tau)(\tau - \bar{\tau})}{(\bar{t} - \tau)^3} \right). \end{aligned} \tag{23}$$

Similarly, from (3), (20), and (21), we have

$$2G(u - iv)_{*c} = \bar{F}d_1(t, \tau) + Fd_2(t, \tau), \tag{24}$$

where

$$\begin{aligned} d_1(t, \tau) &= 2\kappa^2 \ln|t - \bar{\tau}| - (\kappa^2 - 1) \ln(t - \bar{\tau}) - \frac{\tau - \bar{\tau}}{t - \bar{\tau}} + \frac{(\bar{t} - \bar{\tau})(\tau - \bar{\tau})}{(t - \bar{\tau})^2}, \\ d_2(t, \tau) &= -\frac{\kappa(\tau - \bar{\tau})}{\bar{t} - \tau} - \frac{\kappa(\bar{t} - \bar{\tau})}{t - \bar{\tau}}. \end{aligned} \tag{25}$$

In (22) and (24), the subscript  $*c$  denotes that the arguments are derived from the complementary part of the complex potentials. In the functions  $c_1(t, \tau)$ ,  $c_2(t, \tau)$ ,  $d_1(t, \tau)$ , and  $d_2(t, \tau)$ , the variable  $t$  is always located in the upper half-plane and the variable  $\bar{\tau}$  in lower half-plane. Thus, for example, the term  $1/(t - \bar{\tau})$  is regular.

After using Betti’s reciprocal theorem, or the Somigliana identity, between the field of the fundamental solution (or the stress field shown by Figure 2, top left) and the physical field (or the stress field shown by Figure 3), we have

$$P_x u(\tau) + P_y v(\tau) + \text{Re} \left( \int_{\Gamma} (u - iv)(dX + i dY)_{*} \right) = \text{Re} \left( \int_{\Gamma} (u - iv)_{*}(dX + i dY) \right) \quad (\tau \in S^-), \tag{26}$$

where

$$(dX + i dY)_{*} = (dX + i dY)_{*p} + (dX + i dY)_{*c}, \tag{27}$$

$$(u - iv)_{*} = (u - iv)_{*p} + (u - iv)_{*c}. \tag{28}$$

In (26),  $\Gamma$  denotes the notch contour (Figure 3).

In addition, we can define

$$(\sigma_N + i\sigma_{NT})_{*} = (\sigma_N + i\sigma_{NT})_{*p} + (\sigma_N + i\sigma_{NT})_{*c}. \tag{29}$$

In (26), the left-hand term represents the work done by traction in the field of the fundamental solution (Figure 2, top left) to the displacement of the physical field (Figure 3). In addition, the right-hand term represents the work done by traction in the physical field to the displacement in the field of the fundamental solution.



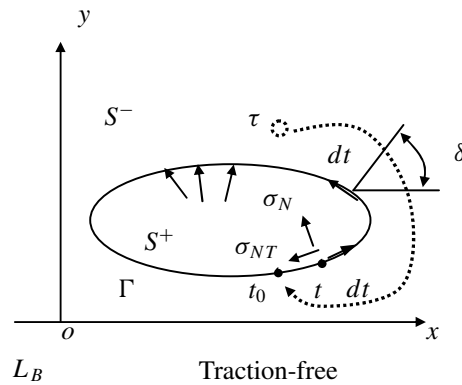


**Figure 3.** A physical stress field for a notch in the half-plane.

In the derivation,  $dX + i dY$  denotes the force applied on the segment  $dt$  (Figures 2 and 3). From Figure 3 or (5), we can find

$$dX + i dY = (\sigma_N + i\sigma_{NT})e^{i(\pi+\delta)} ds = -(\sigma_N + i\sigma_{NT})e^{i\delta} ds = i(\sigma_N + i\sigma_{NT}) dt. \tag{30}$$

By using (27)–(30) and substituting those expressions for  $(\sigma_N + i\sigma_{NT})_{*p}$ ,  $2G(u - iv)_{*p}$ ,  $(\sigma_N + i\sigma_{NT})_{*c}$ , and  $2G(u - iv)_{*c}$  into (26), (26) can be written in an explicit form:

$$\begin{aligned} P_x u(\tau) + P_y v(\tau) + \operatorname{Re} \int_{\Gamma} i \left( \frac{F}{t-\tau} + \frac{\bar{F}}{\bar{t}-\bar{\tau}} + \frac{d\bar{t}}{dt} \left( -\frac{\kappa F}{\bar{t}-\bar{\tau}} - \frac{\bar{F}(t-\tau)}{(\bar{t}-\bar{\tau})^2} \right) \right) (u - iv) dt \\ + \operatorname{Re} \int_{\Gamma} i(\bar{F}c_1(t, \tau) + Fc_2(t, \tau))(u - iv) dt \\ = \frac{1}{2G} \operatorname{Re} \int_{\Gamma} i \left( 2\kappa \bar{F} \ln|t - \tau| - F \frac{\bar{t} - \bar{\tau}}{t - \tau} \right) (\sigma_N + i\sigma_{NT}) dt \\ + \frac{1}{2G} \operatorname{Re} \int_{\Gamma} i(\bar{F}d_1(t, \tau) + Fd_2(t, \tau))(\sigma_N + i\sigma_{NT}) dt, \end{aligned} \tag{31}$$

$\tau \in S^-.$

Note that the point  $\tau (\tau \in S^-)$  now is a domain point (Figure 3).

In the following analysis, one can let

$$U(t) = u(t) + iv(t), \quad Q(t) = \sigma_N(t) + i\sigma_{NT}(t) \quad (t \in \Gamma). \tag{32}$$

In (31), if we let  $P_x = 1, P_y = 0$ , and  $F = -1/2\pi(\kappa + 1)$ , we can find an equation with  $u(\tau)$ . Similarly, if we let  $P_x = 0, P_y = 1$ , and  $F = -i/2\pi(\kappa + 1)$ , we can find an equation with  $v(\tau)$ . Thus, we will find

$$\begin{aligned} u(\tau) + iv(\tau) + B_1 i \int_{\Gamma} \left( -\frac{1}{\bar{t}-\bar{\tau}} + \frac{d\bar{t}}{dt} \frac{(t-\tau)}{(\bar{t}-\bar{\tau})^2} \right) \overline{U(t)} dt + B_1 i \int_{\Gamma} \left( \frac{1}{\bar{t}-\bar{\tau}} - \frac{dt}{d\bar{t}} \frac{\kappa}{t-\tau} \right) U(t) d\bar{t} \\ + B_1 i \int_{\Gamma} C_1(t, \tau) \overline{U(t)} dt + B_1 i \int_{\Gamma} C_2(t, \tau) U(t) d\bar{t} \\ = B_2 i \int_{\Gamma} \left( -2\kappa \ln|t - \tau| Q(t) dt - \frac{t-\tau}{\bar{t}-\bar{\tau}} \overline{Q(t)} d\bar{t} \right) \\ + B_2 i \int_{\Gamma} (D_1(t, \tau) Q(t) dt + D_2(t, \tau) \overline{Q(t)} d\bar{t}), \end{aligned} \tag{33}$$

$\tau \in S^-,$

where

$$C_1(t, \tau) = -c_1(t, \tau) = \frac{\tau - \bar{\tau}}{(t - \bar{\tau})^2} - \frac{\kappa}{\bar{t} - \tau} + \frac{d\bar{t}}{dt} \frac{\kappa(t - \tau)}{(\bar{t} - \tau)^2}, \tag{34}$$

$$C_2(t, \tau) = \overline{c_2(t, \tau)} = \frac{\kappa}{\bar{t} - \tau} - \frac{\tau - \bar{\tau}}{(t - \bar{\tau})^2} + \frac{dt}{d\bar{t}} \left( -\frac{1}{t - \bar{\tau}} - \frac{\tau - \bar{\tau}}{(t - \bar{\tau})^2} + \frac{2(\bar{t} - \bar{\tau})(\tau - \bar{\tau})}{(t - \bar{\tau})^3} \right),$$

$$D_1(t, \tau) = -d_1(t, \tau) = -2\kappa^2 \ln|t - \bar{\tau}| + (\kappa^2 - 1) \ln(t - \bar{\tau}) + \frac{\tau - \bar{\tau}}{t - \bar{\tau}} - \frac{(\bar{t} - \bar{\tau})(\tau - \bar{\tau})}{(t - \bar{\tau})^2}, \tag{35}$$

$$D_2(t, \tau) = \overline{d_2(t, \tau)} = \frac{\kappa(\tau - \bar{\tau})}{t - \bar{\tau}} - \frac{\kappa(t - \tau)}{\bar{t} - \tau},$$

$$B_1 = \frac{1}{2\pi(\kappa + 1)}, \quad B_2 = \frac{1}{4\pi G(\kappa + 1)}. \tag{36}$$

The derivation (31)–(36) is requires care, but not difficult. The relevant derivation can be found in Appendix A.

Equation (33) can be rewritten as

$$\begin{aligned} U(\tau) + B_1 i \int_{\Gamma} \left( -\frac{(\kappa - 1)}{t - \tau} U(t) dt + L_1(t, \tau) U(t) dt - L_2(t, \tau) \overline{U(t)} dt \right) \\ + B_1 i \int_{\Gamma} C_1(t, \tau) \overline{U(t)} dt + B_1 i \int_{\Gamma} C_2(t, \tau) U(t) d\bar{t} \\ = B_2 i \int_{\Gamma} \left( -2\kappa \ln|t - \tau| Q(t) dt - \frac{t - \tau}{\bar{t} - \bar{\tau}} \overline{Q(t)} d\bar{t} \right) \\ + B_2 i \int_{\Gamma} (D_1(t, \tau) Q(t) dt + D_2(t, \tau) \overline{Q(t)} d\bar{t}), \end{aligned} \quad \tau \in S^-, \tag{37}$$

where

$$L_1(t, \tau) = -\frac{d}{dt} \left\{ \ln \frac{t - \tau}{\bar{t} - \bar{\tau}} \right\} = -\frac{1}{t - \tau} + \frac{1}{\bar{t} - \bar{\tau}} \frac{d\bar{t}}{dt}, \quad L_2(t, \tau) = \frac{d}{d\bar{t}} \left\{ \frac{t - \tau}{\bar{t} - \bar{\tau}} \right\} = \frac{1}{\bar{t} - \bar{\tau}} - \frac{t - \tau}{(\bar{t} - \bar{\tau})^2} \frac{d\bar{t}}{d\bar{t}}. \tag{38}$$

In (37), letting  $\tau \rightarrow t_0$  ( $\tau \in S^-$  is a domain point,  $t_0 \in \Gamma$  a boundary point) and using the generalized Sokhotski–Plemelj formulae shown in Appendix B and the results in Appendix C, yields

$$\begin{aligned} \frac{U(t_0)}{2} + B_1 i \int_{\Gamma} \left( -\frac{\kappa - 1}{t - t_0} U(t) dt + L_1(t, t_0) U(t) dt - L_2(t, t_0) \overline{U(t)} dt \right) \\ + B_1 i \int_{\Gamma} C_1(t, t_0) \overline{U(t)} dt + B_1 i \int_{\Gamma} C_2(t, t_0) U(t) d\bar{t} \\ = B_2 i \int_{\Gamma} \left( -2\kappa \ln|t - t_0| Q(t) dt - \frac{t - t_0}{\bar{t} - \bar{t}_0} \overline{Q(t)} d\bar{t} \right) \\ + B_2 i \int_{\Gamma} (D_1(t, t_0) Q(t) dt + D_2(t, t_0) \overline{Q(t)} d\bar{t}), \end{aligned} \quad t_0 \in \Gamma. \tag{39}$$

In (39), the closed elliptic contour  $\Gamma$  corresponds to the closed contour  $L$  shown in Figure 7, middle (see page 978).

Note that, when taking the limit process  $\tau \rightarrow t_0$ , (from  $\tau \in S^-$  to  $t_0 \in \Gamma$ ), the following three integrals in (37),

$$B_1 i \int_{\Gamma} \left(-\frac{(\kappa - 1)}{t - \tau} U(t) dt\right), \quad B_1 i \int_{\Gamma} (L_1(t, \tau) U(t) dt), \quad B_1 i \int_{\Gamma} (-L_2(t, \tau) \overline{U(t)} dt),$$

have jump values  $-\pi B_1(\kappa - 1)U(t_0)$ ,  $-2\pi B_1 U(t_0)$ , and 0, respectively (see the Sokhotski–Plemelj formulae shown in (B.2)–(B.4) in Appendix B and the results in Appendix C). Thus, the three integrals at the left-hand side of (37) have a jump value  $-\pi B_1(\kappa + 1)U(t_0) = -U(t_0)/2$  (equal to the sum of the above-mentioned three values). Finally, the term in (37) becomes  $U(t_0)/2$  (note that  $U(t_0)/2 = U(t_0) - (U(t_0)/2)$ ). In the real variable BIE, this property has been obtained previously [Brebbia et al. 1984]. However, in this paper the property is obtained in a more explicit way by using the generalized Sokhotski–Plemelj formulae shown in (B.2)–(B.4) in Appendix B and the results in Appendix C.

Equation (39) represents the complex variable boundary integral equation for a notch problem in a half-plane with a traction-free boundary of the half-plane, which is based on Betti’s reciprocal theorem or the Somigliana identity. It is seen that the formulation of the fundamental solution is similar to the Green’s function method in the solution of Laplace’s equation.

### 3. Numerical examples

The numerical solution technique is introduced below. After discretization, from (39) the BIE can be written in the form

$$M_U U(t) = M_Q Q(t) \quad (t \text{ denotes the discrete points along notch boundary}), \tag{40}$$

where  $M_U$  is a matrix acting upon the displacement vector  $U(t)$  and  $M_Q$  is a matrix acting upon the traction vector  $Q(t)$ . In the traction boundary value problem, the traction vector  $Q(t)$  is given beforehand, and the displacement vector  $U(t)$  can be evaluated from the algebraic equation derived from (40).

In the computation,  $M$  divisions for the elliptic contour are used. Without loss of generality, one boundary element is assumed on the interval  $|s| \leq d$ . In addition, the following linear shape function for  $U(s)$  (or  $Q(s)$ ) on the interval  $|s| \leq d$  is used:

$$U(s) = f_1 \frac{d-s}{2d} + f_2 \frac{d+s}{2d} \quad (\text{with } U(s)|_{s=-d} = f_1 \text{ and } U(s)|_{s=d} = f_2). \tag{41}$$

Substituting the shape function for  $U(s)$  into the first term of the first integral of (39), if the observation point  $t_0$  is in the middle of the interval, the integral will be reduced to find the following singular integral:

$$\int_{-d}^d \frac{U(s) ds}{s} = f_2 - f_1. \tag{42}$$

In addition, if the point  $t_0$  is located at the middle of the neighboring interval, the relevant integral can be evaluated by some integration rule, for example, the Simpson quadrature rule. In addition, the second and third terms of the first and second integrals in the left-hand side of (39) belong to some regular integral. Those integrals can be integrated by some quadrature rule. Thus, all the elements in the matrix  $M_U$  can be evaluated. Similarly, we can evaluate all the elements in the matrix  $M_Q$ , which is derived from the right-hand side of (39).

Three numerical examples are introduced below. The first example is devoted to examining the efficiency and accuracy of the suggested method, where a known result based on a closed-form solution is obtained in advance. The second example is devoted to evaluating the circumference stress  $\sigma_T$  for an ellipsoidal contour, where some computed results can be compared with those obtained by other researchers. The third example is devoted to evaluating the circumference stress  $\sigma_T$  for a square contour with rounded corners, where the computed results are obtained for the first time in this paper.

**Example 1.** The first example is devoted to examining the efficiency and accuracy of the suggested method. An elliptic notch with two axes  $a$  and  $b$  is located in the upper half-plane, and  $e$  is the distance from the lower edge of the ellipse to the boundary of the half-plane (Figure 4).

The following particular solution is suggested, and the relevant complex potentials take the form

$$\phi(z) = \phi_p(z) + \phi_c(z), \quad \psi(z) = \psi_p(z) + \psi_c(z), \tag{43}$$

where

$$\phi_p(z) = c_1 a^2 p \frac{1}{z - z_c}, \quad \psi_p(z) = c_2 a^2 p \frac{1}{z - z_c}, \tag{44}$$

$$\phi_c(z) = \bar{c}_1 a^2 p \frac{z}{(z - \bar{z}_c)^2} - \bar{c}_2 a^2 p \frac{1}{z - \bar{z}_c}, \quad \psi_c(z) = \bar{c}_1 a^2 p \left( -\frac{1}{z - \bar{z}_c} + \frac{z(z + \bar{z}_c)}{(z - \bar{z}_c)^3} \right) - \bar{c}_2 a^2 p \frac{z}{(z - \bar{z}_c)^2}, \tag{45}$$

with  $z_c = (b + e)i = hi$ .

In (44) and (46),  $c_1$  and  $c_2$  are some constants, and  $p$  denotes some parameter which has dimensions of stress. The tractions applied on the elliptic contour can be evaluated from (1) accordingly (Figure 4). In addition,  $b/a = 0.5$ ,  $e/b = 0.2$ ,  $c_1 = 1 + 0.5i$ , and  $c_2 = 2 + 1.5i$  are used in computation. It is easy to verify that the complex potentials shown by (43)–(45) satisfy the traction-free condition along the boundary of the half-plane (or  $L_b$ ). The derivation for  $\phi_c(z)$  and  $\psi_c(z)$  from the assumed  $\phi_p(z)$  and  $\psi_p(z)$  can be found in [Chen and Cheung 1990; Chen et al. 2003; 2009].

As mentioned above, after discretization to (39), the BIE can be written in the form

$$\mathbf{M}_U \mathbf{U}(t) = \mathbf{M}_Q \mathbf{Q}(t) \quad (t \text{ denoting the discrete points}), \tag{46}$$

where  $\mathbf{M}_U$  is a matrix acting upon the displacement vector  $\mathbf{U}(t)$ , and  $\mathbf{M}_Q$  is a matrix acting upon the traction vector  $\mathbf{Q}(t)$ . In the computation,  $M = 180$  divisions for the elliptic contour are used in computation.

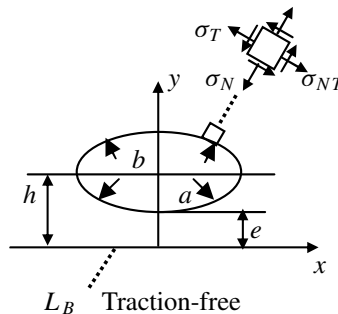


**Figure 4.** An elliptic notch in the half-plane under some loading along the notch contour.

In the examination,  $U_{\text{ex}}$  ( $Q_{\text{ex}}$ ) denotes the displacement (traction) obtained from the exact solution with the complex potentials shown by (43)–(45). In the meantime,  $U_{\text{num}}$  ( $Q_{\text{num}}$ ) denotes the displacement (traction) obtained from a numerical solution.

In the examination of the Dirichlet problem, from the input data  $U_{\text{ex}}(t)$  and (46), the following algebraic equation is obtained:

$$\mathbf{M}_Q \mathbf{Q}(t) = \mathbf{M}_U U_{\text{ex}}(t). \quad (47)$$

From (47), we can obtain the numerical solution for the vector  $Q_{\text{num}}(t)$ . In addition, the numerical solution  $Q_{\text{num}}(t)$  is compared with the exact one. After computation, we find the error

$$\frac{\max|Q_{\text{num}}(t_j) - Q_{\text{ex}}(t_j)|}{\max|Q_{\text{ex}}(t_j)|} = 0.23\%$$

from many discrete points.

In the examination of the Neumann problem, from the input data  $Q_{\text{ex}}(t)$  and (46), the following algebraic equation is obtained:

$$\mathbf{M}_U \mathbf{U}(t) = \mathbf{M}_Q \mathbf{Q}_{\text{ex}}(t). \quad (48)$$

From (48), we can obtain the numerical solution for the vector  $U_{\text{num}}(t)$ . In addition, the numerical solution  $U_{\text{num}}(t)$  is compared with the exact one. After computation, we find the error

$$\frac{\max|U_{\text{num}}(t_j) - U_{\text{ex}}(t_j)|}{\max|U_{\text{ex}}(t_j)|} = 1.11\%$$

from many discrete points.

For the examination of the circumference stress  $\sigma_T$  component, the following technique is suggested. In the plane strain case, the strain component  $\epsilon_T$  (in the  $T$  direction) can be expressed as (see Figure 4)

$$\epsilon_T = \frac{1}{E} (\sigma_T(1 - \nu^2) - \nu(1 + \nu)\sigma_N), \quad (49)$$

or

$$\sigma_T = \frac{E\epsilon_T + \nu(1 + \nu)\sigma_N}{1 - \nu^2}, \quad (50)$$

where  $E$  is the Young's modulus of elasticity. In (49), the component  $\sigma_N$  is from input data, and  $\epsilon_T$  is the strain in the  $T$  direction which can be evaluated from the obtained displacement on the boundary. Thus, the values of  $\sigma_T$  at discrete points are obtainable.

In addition, the numerical solution  $\sigma_{T,\text{num}}(t)$  is compared with the exact one. After computation, we find the error  $\max|\sigma_{T,\text{num}}(t_j) - \sigma_{T,\text{ex}}(t_j)| / \max|\sigma_{T,\text{ex}}(t_j)| = 1.17\%$  from many discrete points. From the above-mentioned results we see that the suggested technique provides an accurate result in this example.

**Example 2.** The second example is devoted to evaluating the circumference stress  $\sigma_T$  for an elliptic contour with two axes  $a$  and  $b$  located in the upper half-plane, where  $e$  is the distance from the lower edge of the ellipse to the boundary of the half-plane (Figure 5). The remote loading is  $\sigma_x = p$ , and the boundary of the half-plane is traction-free. As before,  $M = 180$  divisions are used in the discretization.

The normalized stress is denoted by  $f_T$  ( $f_T = \sigma_T/p$ ). Table 1 shows the computed results for  $f_T$  ( $f_T = \sigma_T/p$ ) under the following conditions:

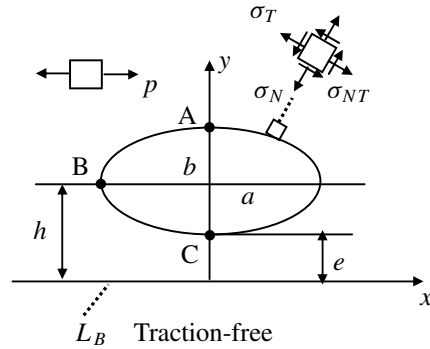


**Figure 5.** An elliptic notch in the half-plane under the remote tension  $\sigma_x = p$ .

<i>b/a = 0.5</i>										
Point	<i>e/b = 0.1</i>	0.2	0.3	0.4	0.5	0.6	0.7	0.8	0.9	1
A	2.361	2.307	2.270	2.243	2.221	2.202	2.187	2.173	2.161	2.151
B	-0.681	-0.945	-1.092	-1.183	-1.239	-1.275	-1.296	-1.308	-1.314	-1.315
C	7.178	5.154	4.358	3.890	3.573	3.342	3.163	3.021	2.905	2.808
	<i>e/b = 1</i>	2	3	4	5	6	7	8	9	10
A	2.151	2.090	2.058	2.040	2.031	2.024	2.022	2.018	2.016	2.014
B	-1.315	-1.246	-1.173	-1.123	-1.096	-1.069	-1.056	-1.045	-1.036	-1.030
C	2.808	2.327	2.170	2.100	2.070	2.049	2.038	2.029	2.024	2.020
<i>b/a = 1</i>										
Point	<i>e/b = 0.1</i>	0.2	0.3	0.4	0.5	0.6	0.7	0.8	0.9	1
A	3.626	3.510	3.435	3.381	3.338	3.303	3.275	3.250	3.229	3.211
B	-0.840	-1.035	-1.129	-1.178	-1.203	-1.214	-1.217	-1.215	-1.210	-1.203
C	9.314	6.739	5.659	5.040	4.632	4.344	4.128	3.961	3.830	3.724
	<i>e/b = 1</i>	2	3	4	5	6	7	8	9	10
A	3.211	3.110	3.064	3.040	3.031	3.024	3.026	3.022	3.019	3.017
B	-1.203	-1.124	-1.075	-1.048	-1.038	-1.026	-1.024	-1.020	-1.016	-1.014
C	3.724	3.253	3.128	3.071	3.055	3.039	3.033	3.027	3.023	3.019
<i>b/a = 2</i>										
Point	<i>e/b = 0.1</i>	0.2	0.3	0.4	0.5	0.6	0.7	0.8	0.9	1
A	6.096	5.864	5.720	5.617	5.539	5.477	5.426	5.384	5.348	5.317
B	-0.946	-1.080	-1.133	-1.154	-1.159	-1.157	-1.152	-1.144	-1.136	-1.128
C	12.893	9.415	8.027	7.264	6.778	6.443	6.200	6.013	5.870	5.756
	<i>e/b = 1</i>	2	3	4	5	6	7	8	9	10
A	5.317	5.148	5.083	5.049	5.039	5.031	5.041	5.036	5.032	5.029
B	-1.128	-1.065	-1.037	-1.022	-1.020	-1.015	-1.017	-1.015	-1.013	-1.012
C	5.756	5.263	5.136	5.074	5.066	5.048	5.046	5.039	5.035	5.031

**Table 1.** The normalized circumference stress  $f_T$  ( $f_T = \sigma_T/p$ ) at some points for an elliptic notch (see Figure 5).

- (1)  $b/a = 0.5, 1, 2,$
- (2)  $e/b = 0.1, 0.2, \dots 1$  and  $1, 2, \dots 10,$  and
- (3) at the boundary points A, B, and C (Figure 5),

From Table 1 we see that, for the small  $e/b$  case, the stress concentration factor can reach a larger value. For example, for the following three cases:

- (1)  $e/b = 0.1, b/a = 0.5,$
- (2)  $e/b = 0.1, b/a = 1.0,$  and
- (3)  $e/b = 0.1, b/a = 2,$

at the point C we have  $f_T$  values 7.178, 9.314, and 12.893, respectively.

For purposes of comparison, the computed results for  $f_T$  under the condition  $b/a = 1$  and  $e/b = 0.185, 0.337, 0.543, 0.811, 1.151, 1.577, 2.107,$  and  $2.762$  are plotted in Table 2. It is found from the tabulated results that the computed results coincide with those obtained in [Dejoie et al. 2006].

**Example 3.** The third example is devoted to evaluating the circumference stress  $\sigma_T$  for a square contour with rounded corners. The width of the square contour is  $2a,$  and the radius of the rounded corners is  $0.5a$  (Figure 6). Under the conditions:

- (1)  $e/a = 0.1, 0.2, \dots, 1,$  and  $1, 2, \dots, 10$  and
- (2) at the boundary points A, B, C, D, and E,

the computed results for  $f_T$  ( $f_T = \sigma_T/p$ ) are plotted in Table 3.

From Table 3 we see that, for the small  $e/b$  case, the stress concentration factor can reach a larger value. For example, for the two cases  $e/a = 0.1$  and  $0.2,$  at the point E we have  $f_T$  values 5.213 and 4.212, respectively.

Point	$e/b = 0.185$	0.337	0.543	0.811	1.151	1.577	2.107	2.762
A*	3.520	3.413	3.321	3.248	3.188	3.141	3.102	3.079
A*1	3.524	3.414		3.249		3.142	3.104	3.076
A*2	3.293	3.302	3.274	3.229	3.181	3.139	3.103	3.075
A*3	3.362	3.266	3.201	3.152	3.115	3.087	3.065	3.048
B*	-1.012	-1.146	-1.205	-1.211	-1.191	-1.156	-1.122	-1.090
B*1	-1.104	-1.151		-1.215		-1.157	-1.121	-1.089
B*2	-0.730	-1.010	-1.148	-1.190	-1.182	-1.153	-1.119	-1.089
C*	6.975	5.388	4.492	3.941	3.598	3.377	3.242	3.153
C*1	6.960	5.390		3.944		3.377	3.238	3.151
C*2	5.614	4.982	4.365	3.900	3.581	3.372	3.236	3.150
C*3	5.064	4.366	3.919	3.609	3.396	3.254	3.162	3.108

**Table 2.** Comparison results for the normalized circumference stress  $f_T = \sigma_T/p$  at some points for a circular hole ( $b/a = 1$ ). See Figure 5. \* indicates data from the present study, \*1 from [Dejoie et al. 2006], \*2 from [Chen 1994], and \*3 from [Savin 1961].

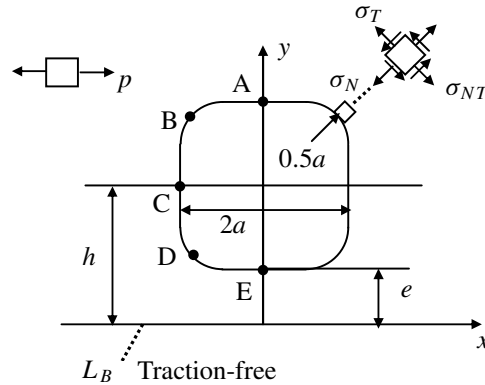


**Figure 6.** A square notch with rounded corners in the half-plane under the remote tension  $\sigma_x = p$ .

Point	$e/b = 0.1$	0.2	0.3	0.4	0.5	0.6	0.7	0.8	0.9	1
A	2.328	2.242	2.191	2.154	2.130	2.109	2.092	2.078	2.066	2.056
B	2.544	2.315	2.173	2.073	2.000	1.942	1.895	1.858	1.827	1.800
C	-0.483	-0.662	-0.751	-0.801	-0.828	-0.844	-0.852	-0.855	-0.855	-0.854
D	-1.427	-0.668	-0.123	0.245	0.504	0.693	0.837	0.952	1.043	1.117
E	5.213	4.212	3.703	3.378	3.141	2.959	2.813	2.696	2.598	2.517
Point	$e/b = 1$	2	3	4	5	6	7	8	9	10
A	2.056	1.992	1.967	1.953	1.940	1.937	1.928	1.925	1.923	1.921
B	1.800	1.669	1.627	1.609	1.595	1.591	1.584	1.582	1.581	1.580
C	-0.854	-0.818	-0.789	-0.773	-0.768	-0.765	-0.765	-0.762	-0.759	-0.758
D	1.117	1.446	1.527	1.558	1.565	1.573	1.572	1.574	1.575	1.575
E	2.517	2.143	2.031	1.985	1.956	1.946	1.936	1.931	1.927	1.925

**Table 3.** The normalized circumference stress  $f_T$  ( $f_T = \sigma_T/p$ ) at some points for a square notch with rounded corners (see Figure 6).

#### 4. Conclusions

Formulation of the fundamental solution based on Green’s function method plays an important role in the present study. Since two stress fields for the fundamental solution and for the physical problem satisfy the traction-free condition along the boundary of the half-plane, we can formulate the BIE on the boundary of the notch only. In addition, the computed results for the case of a circular hole prove that the suggested BIE provides accurate results.

#### Appendix A: Derivation of (33) from (31)

The following is useful for the derivation of (33) from (31). We may assume a value as follows:

$$C = \text{Re}(i\bar{H}s) \quad (\text{where } H = -P_x - iP_y \text{ and } s \text{ is a complex value}). \tag{A.1}$$



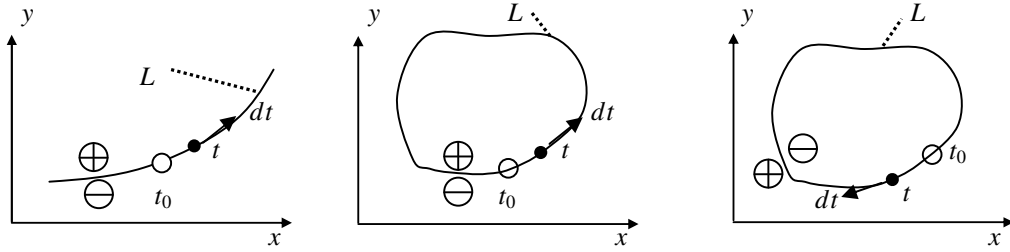


**Figure 7.** Left: a curve  $L$  in an infinite plane. Middle: a closed contour  $L$  in an infinite plane with  $dt$  in the counterclockwise direction. Right: a closed contour  $L$  in an infinite plane with  $dt$  in the clockwise direction.

Thus, we will find

$$C|_{P_x=1, P_y=0} + iC|_{P_x=0, P_y=1} = \operatorname{Re}(-is) + i \operatorname{Re}(-s) = \operatorname{Re}(-is) + i \operatorname{Im}(-is) = -is. \tag{A.2}$$

For example, one term in (31) can be expressed as follows:

$$S = \frac{1}{2G} \operatorname{Re} \int_{\Gamma} i(2k\bar{F} \ln|t - \tau|)(\sigma_N + i\sigma_{NT}) dt = B_2 \operatorname{Re} \int_{\Gamma} i\bar{H}(2k \ln|t - \tau|)(\sigma_N + i\sigma_{NT}) dt. \tag{A.3}$$

By using (A.2), we have

$$S|_{P_x=1, P_y=0} + iS|_{P_x=0, P_y=1} = B_2i \int_{\Gamma} (-2k \ln|t - \tau|)(\sigma_N + i\sigma_{NT}) dt. \tag{A.4}$$

Similarly, we can assume

$$D = \operatorname{Re}(iHt) \quad (\text{where } H = -P_x - iP_y, \text{ and } t \text{ is a complex value}). \tag{A.5}$$

Similarly, we have

$$D|_{P_x=1, P_y=0} + iD|_{P_x=0, P_y=1} = \operatorname{Re}(-it) + i \operatorname{Re}(t) = \operatorname{Re}(i\bar{t}) + i \operatorname{Re}(\bar{t}) = \operatorname{Re}(i\bar{t}) + i \operatorname{Im}(i\bar{t}) = i\bar{t}. \tag{A.6}$$

For example, one term in (31) can be expressed as follows:

$$T = \frac{1}{2G} \operatorname{Re} \int_{\Gamma} i\left(-F \frac{\bar{t} - \bar{\tau}}{t - \tau}\right)(\sigma_N + i\sigma_{NT}) dt = B_2 \operatorname{Re} \int_{\Gamma} i\left(-H \frac{\bar{t} - \bar{\tau}}{t - \tau}\right)(\sigma_N + i\sigma_{NT}) dt. \tag{A.7}$$

By using (A.6), we have

$$T|_{P_x=1, P_y=0} + iT|_{P_x=0, P_y=1} = B_2i \int_{\Gamma} -\frac{t - \tau}{\bar{t} - \bar{\tau}}(\sigma_N - i\sigma_{NT}) d\bar{t}. \tag{A.8}$$

### Appendix B: The generalized Sokhotski–Plemelj formulae

In plane elasticity, the following integrals are useful [Muskhelishvili 1953; Savruk 1981; Chen et al. 2003]:

$$F(z) = \frac{1}{2\pi i} \int_L \frac{f(t) dt}{t - z}, \quad G(z) = \frac{1}{2\pi i} \int_L \frac{g(t) d\bar{t}}{t - z}, \quad H(z, \bar{z}) = \frac{1}{2\pi i} \int_L \frac{\bar{t} - \bar{z}}{(t - z)^2} h(t) dt, \tag{B.1}$$

where  $L$  is a smooth curve or a closed contour as shown in Figure 7, and the integrals should be understood in the sense of the principal value. Also, we assume that the functions  $f(t)$ ,  $g(t)$ , and  $h(t)$  satisfy the Hölder condition [Muskhelishvili 1953]. Sometimes, the functions  $f(t)$ ,  $g(t)$ , and  $h(t)$  are called the density functions hereafter. Clearly, the first two integrals in (B.1) are analytic functions, and the last one is not. The first integral in (B.1) is the well-known Cauchy integral.

Generally speaking, these integrals take different values when  $z \rightarrow t_0^+$  and  $z \rightarrow t_0^-$  ( $t_0 \in L$ ). The limit values of these functions from the upper and lower sides of the curve  $L$  are found to be [Muskhelishvili 1953; Savruk 1981; Chen et al. 2003]

$$F^\pm(t_0) = \pm \frac{f(t_0)}{2} + \frac{1}{2\pi i} \int_L \frac{f(t) dt}{t - t_0}, \tag{B.2}$$

$$G^\pm(t_0) = \pm \frac{g(t_0)}{2} \frac{d\bar{t}_0}{dt_0} + \frac{1}{2\pi i} \int_L \frac{g(t) d\bar{t}}{t - t_0}, \tag{B.3}$$

$$H^\pm(t_0, \bar{t}_0) = \pm \frac{h(t_0)}{2} \frac{d\bar{t}_0}{dt_0} + \frac{1}{2\pi i} \int_L \frac{\bar{t} - \bar{t}_0}{(t - t_0)^2} h(t) dt. \tag{B.4}$$

Note that the notations  $f(t)$ ,  $g(t)$ ,  $h(t)$ ,  $F(z)$ ,  $G(z)$ , and  $H(z, \bar{z})$  used in (B.1) have no relation with those mentioned in other places.

**Appendix C: Properties of some integrals  
with kernel functions  $L_1(t, z)$  and  $L_2(t, z)$  defined by (38)**

The two integrals with kernel functions  $L_1(t, z)$  and  $L_2(t, z)$  shown by (38) are written in the form

$$W_1(z) = \frac{1}{2\pi i} \int_\Gamma L_1(t, z) f(t) dt \quad (z \in S^+ \text{ or } z \in S^-), \tag{C.1}$$

$$W_2(z) = \frac{1}{2\pi i} \int_\Gamma L_2(t, z) f(t) dt \quad (z \in S^+ \text{ or } z \in S^-), \tag{C.2}$$

where

$$L_1(t, z) = -\frac{d}{dt} \left\{ \ln \frac{t - z}{\bar{t} - \bar{z}} \right\} = -\frac{1}{t - z} + \frac{1}{\bar{t} - \bar{z}} \frac{d\bar{t}}{dt}, \tag{C.3}$$

$$L_2(t, z) = \frac{d}{dt} \left\{ \frac{t - z}{\bar{t} - \bar{z}} \right\} = \frac{1}{\bar{t} - \bar{z}} - \frac{t - z}{(\bar{t} - \bar{z})^2} \frac{d\bar{t}}{dt}. \tag{C.4}$$

In (C.1) and (C.2),  $\Gamma$  denotes a closed contour and  $f(t)$  is an arbitrary function. If  $dt$  goes forward in a counterclockwise direction,  $S^+$  and  $S^-$  are the inside finite region and outside infinite region, respectively (Figure 3).

In (C.1) and (C.2), letting  $z \rightarrow t_0$  ( $z \in S^+$ ,  $t_0 \in \Gamma$ ) and  $z \rightarrow t_0$  ( $z \in S^-$ ,  $t_0 \in \Gamma$ ), and using the generalized Sokhotski–Plemelj formulae shown in Appendix B, we will find

$$W_1^\pm(t_0) = \mp f(t_0) + \frac{1}{2\pi i} \int_\Gamma L_1(t, t_0) f(t) dt \quad (t_0 \in \Gamma), \tag{C.5}$$

$$W_2^\pm(t_0) = \frac{1}{2\pi i} \int_\Gamma L_2(t, t_0) f(t) dt \quad (t_0 \in \Gamma). \tag{C.6}$$

We can prove the assertion shown by (C.5) as follows. In fact, we can rewrite  $W_1(z)$  as

$$W_1(z) = I_1 + I_2 \quad (z \in S^+ \text{ or } z \in S^-), \quad (\text{C.7})$$

where

$$I_1(z) = \frac{1}{2\pi i} \int_{\Gamma} \left(-\frac{1}{t-z}\right) f(t) dt \quad (z \in S^+ \text{ or } z \in S^-), \quad (\text{C.8})$$

$$I_2(z) = \frac{1}{2\pi i} \int_{\Gamma} \left(\frac{1}{\bar{t}-\bar{z}} \frac{d\bar{t}}{dt}\right) f(t) dt \quad (z \in S^+ \text{ or } z \in S^-). \quad (\text{C.9})$$

For convenience in derivation, we can define

$$I_3(z) = -\overline{I_2(z)} = \frac{1}{2\pi i} \int_{\Gamma} \frac{1}{t-z} \overline{f(t)} dt \quad (z \in S^+ \text{ or } z \in S^-). \quad (\text{C.10})$$

In (C.8) and (C.10), letting  $z \rightarrow t_0$  ( $z \in S^+$ ,  $t_0 \in \Gamma$ ) and  $z \rightarrow t_0$  ( $z \in S^-$ ,  $t_0 \in \Gamma$ ), and using the generalized Sokhotski–Plemelj formulae shown in Appendix B, we will find

$$I_1^{\pm}(t_0) = \mp \frac{f(t_0)}{2} + \frac{1}{2\pi i} \int_{\Gamma} \frac{-1}{t-t_0} f(t) dt \quad (t_0 \in \Gamma), \quad (\text{C.11})$$

$$I_3^{\pm}(t_0) = -\overline{I_2^{\pm}(t_0)} = \pm \frac{\overline{f(t_0)}}{2} + \frac{1}{2\pi i} \int_{\Gamma} \frac{1}{t-t_0} \overline{f(t)} dt \quad (t_0 \in \Gamma). \quad (\text{C.12})$$

In addition, from (C.10) and (C.12) we will find

$$I_2^{\pm}(t_0) = -\overline{I_3^{\pm}(t_0)} = \mp \frac{f(t_0)}{2} + \frac{1}{2\pi i} \int_{\Gamma} \left(\frac{1}{\bar{t}-\bar{t}_0} \frac{d\bar{t}}{dt}\right) f(t) dt \quad (t_0 \in \Gamma). \quad (\text{C.13})$$

From (C.7), (C.11), and (C.13), the validity of (C.5) is proved. Similarly, we can prove the validity of (C.6).

### Acknowledgment

The author is grateful to the reviewers for their valuable comments and suggestions on the original manuscript.

### References

- [Brebbia et al. 1984] C. A. Brebbia, J. C. F. Telles, and L. C. Wrobel, *Boundary element techniques: theory and applications in engineering*, Springer, Heidelberg, 1984.
- [Chen 1985] Y. Z. Chen, “A special boundary-element formulation for multiple-circular-hole problems in an infinite plate”, *Comput. Methods Appl. Mech. Eng.* **50**:3 (1985), 263–273.
- [Chen 1994] Y. Z. Chen, “Multiple circular hole problem for an elastic half-plane”, *Comput. Struct.* **52** (1994), 1277–1281.
- [Chen and Chen 2004] J. T. Chen and Y. W. Chen, “Dual boundary element analysis using complex variables for potential problems with or without a degenerate boundary”, *Eng. Anal. Bound. Elem.* **24** (2004), 671–684.
- [Chen and Cheung 1990] Y. Z. Chen and Y. K. Cheung, “New integral equation approach for the crack problem in elastic half-plane”, *Int. J. Fract.* **46** (1990), 57–69.
- [Chen and Lin 2007] Y. Z. Chen and X. Y. Lin, “Solution of periodic group circular hole problems by using series expansion variational method”, *Int. J. Numer. Methods Eng.* **69** (2007), 1405–1422.

- [Chen et al. 2003] Y. Z. Chen, N. Hasebe, and K. Y. Lee, *Multiple crack problems in elasticity*, Advances in Damage Mechanics **4**, WIT Press, Southampton, 2003.
- [Chen et al. 2009] Y. Z. Chen, X. Y. Lin, and Z. X. Wang, “Numerical solution for curved crack problem in elastic half-plane using hypersingular integral equation”, *Philos. Mag.* **86** (2009), 2239–2253.
- [Chen et al. 2010] Y. Z. Chen, X. Y. Lin, and Z. X. Wang, “Formulation of indirect BIEs in plane elasticity using single or double layer potentials and complex variable”, *Eng. Anal. Bound. Elem.* **34**:4 (2010), 337–351.
- [Cheng and Cheng 2005] A. H. D. Cheng and D. T. Cheng, “Heritage and early history of the boundary element method”, *Eng. Anal. Bound. Elem.* **29** (2005), 268–302.
- [Cruse 1969] T. A. Cruse, “Numerical solutions in three-dimensional elastostatics”, *Int. J. Solids Struct.* **5** (1969), 1259–1274.
- [Dejoie et al. 2006] A. Dejoie, S. G. Mogilevskaya, and S. L. Crouch, “A boundary integral method for multiple circular holes in an elastic half-plane”, *Eng. Anal. Bound. Elem.* **30** (2006), 450–464.
- [Hong and Chen 1988] H. K. Hong and J. T. Chen, “Derivations of integral equations of elasticity”, *J. Eng. Mech. (ASCE)* **114** (1988), 1028–1044.
- [Hromadka and Lai 1987] T. V. Hromadka, II and C. Lai, *The complex variable boundary element method in engineering analysis*, Springer, New York, 1987.
- [Jaswon and Symm 1977] M. A. Jaswon and G. T. Symm, *Integral equation methods in potential theory and elastostatics*, Academic Press, London, 1977.
- [Linkov 2002] A. M. Linkov, *Boundary integral equations in elasticity theory*, Solid Mechanics and its Applications **99**, Kluwer, Dordrecht, 2002.
- [Linkov and Mogilevskaya 1994] A. M. Linkov and S. G. Mogilevskaya, “Complex hypersingular integrals and integral equations in plane elasticity”, *Acta Mech.* **105**:1-4 (1994), 189–205.
- [Mogilevskaya and Linkov 1998] S. G. Mogilevskaya and A. M. Linkov, “Complex fundamental solutions and complex variables boundary element method in elasticity”, *Comput. Mech.* **22**:1 (1998), 88–92.
- [Muskhelishvili 1953] N. I. Muskhelishvili, *Some basic problems of the mathematical theory of elasticity*, Noordhoff, Groningen, 1953.
- [Pan et al. 1997] E. Pan, C. S. Chen, and B. Amadei, “A BEM formulation for anisotropic half-plane problems”, *Eng. Anal. Bound. Elem.* **20** (1997), 185–195.
- [Rizzo 1967] F. J. Rizzo, “An integral equation approach to boundary value problems in classical elastostatics”, *Quart. Appl. Math.* **25** (1967), 83–95.
- [Savin 1961] G. N. Savin, *Stress concentration around holes*, International Series of Monographs in Aeronautics and Astronautics, Division I: Solid and Structural Mechanics **1**, Pergamon, New York, 1961.
- [Savruk 1981] M. P. Savruk, *Двухмерные задачи упругости для тел с трещинами*, Naukova Dumka, Kiev, 1981.
- [Verruijt 1998] A. Verruijt, “Deformations of an elastic half plane with a circular cavity”, *Int. J. Solids Struct.* **35** (1998), 2795–2804.
- [Wang et al. 2003] J. L. Wang, S. L. Crouch, and S. G. Mogilevskaya, “A complex boundary integral method for multiple circular holes in an infinite plane”, *Eng. Anal. Bound. Elem.* **27** (2003), 789–802.

Received 1 Sep 2012. Revised 20 Oct 2012. Accepted 26 Oct 2012.

Y. Z. CHEN: chens@ujs.edu.cn

Division of Engineering Mechanics, Jiangsu University, Xue Fu Road 301, Zhenjiang, Jiangsu 212013, China

# JOURNAL OF MECHANICS OF MATERIALS AND STRUCTURES

[msp.org/jomms](http://msp.org/jomms)

Founded by Charles R. Steele and Marie-Louise Steele

## EDITORS

CHARLES R. STEELE Stanford University, USA  
DAVIDE BIGONI University of Trento, Italy  
IWONA JASIUK University of Illinois at Urbana-Champaign, USA  
YASUhide SHINDO Tohoku University, Japan

## EDITORIAL BOARD

H. D. BUI École Polytechnique, France  
J. P. CARTER University of Sydney, Australia  
R. M. CHRISTENSEN Stanford University, USA  
G. M. L. GLADWELL University of Waterloo, Canada  
D. H. HODGES Georgia Institute of Technology, USA  
J. HUTCHINSON Harvard University, USA  
C. HWU National Cheng Kung University, Taiwan  
B. L. KARIHALOO University of Wales, UK  
Y. Y. KIM Seoul National University, Republic of Korea  
Z. MROZ Academy of Science, Poland  
D. PAMPLONA Universidade Católica do Rio de Janeiro, Brazil  
M. B. RUBIN Technion, Haifa, Israel  
A. N. SHUPIKOV Ukrainian Academy of Sciences, Ukraine  
T. TARNAI University Budapest, Hungary  
F. Y. M. WAN University of California, Irvine, USA  
P. WRIGGERS Universität Hannover, Germany  
W. YANG Tsinghua University, China  
F. ZIEGLER Technische Universität Wien, Austria

**PRODUCTION** [production@msp.org](mailto:production@msp.org)

SILVIO LEVY Scientific Editor

---

See [msp.org/jomms](http://msp.org/jomms) for submission guidelines.

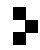
---

JoMMS (ISSN 1559-3959) at Mathematical Sciences Publishers, 798 Evans Hall #6840, c/o University of California, Berkeley, CA 94720-3840, is published in 10 issues a year. The subscription price for 2012 is US \$555/year for the electronic version, and \$735/year (+\$60, if shipping outside the US) for print and electronic. Subscriptions, requests for back issues, and changes of address should be sent to MSP.

---

JoMMS peer-review and production is managed by EditFLOW® from Mathematical Sciences Publishers.

PUBLISHED BY

 **mathematical sciences publishers**  
nonprofit scientific publishing

<http://msp.org/>

© 2012 Mathematical Sciences Publishers

# Journal of Mechanics of Materials and Structures

Volume 7, No. 10

December 2012

- 
- Indentation and residual stress in the axially symmetric elastoplastic contact problem** TIAN-HU HAO 887
- Form finding of tensegrity structures using finite elements and mathematical programming**  
KATALIN K. KLINKA, VINICIUS F. ARCARO and DARIO GASPARINI 899
- Experimental and analytical investigation of the behavior of diaphragm-through joints of concrete-filled tubular columns** RONG BIN, CHEN ZHIHUA, ZHANG RUOYU, APOSTOLOS FAFITIS and YANG NAN 909
- Buckling and postbuckling behavior of functionally graded Timoshenko microbeams based on the strain gradient theory**  
REZA ANSARI, MOSTAFA FAGHIH SHOJAEI, VAHID MOHAMMADI, RAHEB GHOLAMI and MOHAMMAD ALI DARABI 931
- Measurement of elastic properties of AISI 52100 alloy steel by ultrasonic nondestructive methods**  
MOHAMMAD HAMIDNIA and FARHANG HONARVAR 951
- Boundary integral equation for notch problems in an elastic half-plane based on Green's function method** Y. Z. CHEN 963
- Internal structures and internal variables in solids**  
JÜRI ENGELBRECHT and ARKADI BEREZOVSKI 983
- The inverse problem of seismic fault determination using part time measurements**  
HUY DUONG BUI, ANDREI CONSTANTINESCU and HUBERT MAIGRE 997



1559-3959(2012)7:10;1-#